Charge Recombination Fluorescence in Photosystem I Reaction Centers from *Chlamydomonas reinhardtii*

Alfred R. Holzwarth,* Marc G. Müller, Jens Niklas, and Wolfgang Lubitz

Max-Planck-Institut für Bioanorganische Chemie, Stiftstr. 34-36, D-45470 Mülheim a.d. Ruhr, Germany

Received: August 17, 2004; In Final Form: January 24, 2005

The fluorescence kinetics of photosystem I core particles from *Chlamydomonas reinhardtii* have been measured with picosecond resolution in order to test a previous hypothesis suggesting a charge recombination mechanism for the early electron-transfer steps and the fluorescence kinetics (Müller et al. *Biophys. J.* **2003**, *85*, 3899−3922). Performing global target analyses for various kinetic models on the original fluorescence data confirms the "charge recombination" model as the only acceptable one of the models tested while all of the other models can be excluded. The analysis allowed a precise determination of (i) the effective charge separation rate constant from the equilibrated reaction center excited state (438 ns^{-1}) confirming our previous assignment based on transient absorption data (Müller et al. *Biophys. J.* **2003**, *85*, 3899−3922), (ii) the effective charge recombination rate constant back to the excited state (52 ns^{-1}), and (iii) the intrinsic secondary electron-transfer rate constant (80 ns^{-1}). The average energy equilibration lifetime core antenna/RC is about 1 ps in the "charge recombination" model, in agreement with previous transient absorption data, vs the 18−20 ps energy transfer lifetime from antenna to RC within "transfer-to-the-trap-limited" models. The apparent charge separation lifetime in the recombination model is about three times faster than in the "transfer-to-the-trap-limited" model. We conclude that the charge separation kinetics is trap-limited in PS I cores devoid of red antenna states such as in *C. reinhardtii*.

Introduction

Photosystem I (PS I) is one of the two photosystems of oxygenic photosynthetic organisms which are connected by the sequential Z-scheme mechanism for electron transfer. PS I receives electrons from the plastoquinone pool on the acceptor side, and its physiological function is to catalyze light-driven transfer of electrons from reduced plastocyanin or cytochrome c_6 located in the lumen to ferredoxin in the stroma (see ref 1 for a review). High-resolution X-ray structures exist for both cyanobacterial PS I[2,3] as well as for higher plant PS I.[4] The higher plant PS I is monomeric and contains 93 Chls in the core, including the reaction center (RC), with the remainder of the total 167 Chls located in four peripheral light-harvesting complexes (LHC I).[4] The core of cyanobacterial PS I is organized as a trimer, comprising 96 Chls per monomer, and lacks peripheral antennae.[2] The core structure is highly conserved between the two types of organisms.

The mechanism and kinetics of the early ultrafast events of energy transfer from the antenna to the RC and for the electron transfer within the RC are still a matter of intensive debate. Since the antenna Chls and the RC Chls are both bound to the same polypeptide units,[2] the electron transfer processes cannot be studied separately from the energy transfer processes since an intact well-defined PS I RC devoid of antenna Chls cannot be isolated. Thus, the energy transfer from the antenna to the RC and the electron transfer dynamics are tightly linked processes which presents a key difficulty in the interpretation of optical kinetic data (see however refs 5 and 6 for studies of the RC kinetics in PS I preparations with reduced antenna size). The problem is aggravated further by the fact that energy and electron-transfer processes occur on comparable picosecond time scales.

On the basis of femtosecond transient absorption data of PS I cores of the green algae *C. reinhardtii*, we recently showed that both the energy transfer from the core antenna to the RC as well as the primary electron transfer process occur much faster than previously assumed[7] (see that paper also for an extensive discussion of the problems with previous kinetic and mechanistic interpretations of the PS I kinetics). We proposed a new model for the energy transfer and early electron-transfer processes where the energy equilibration between the PS I core antenna and the RC occurs with lifetimes of 1−2 ps and the apparent primary charge separation lifetime is about 7−9 ps[7] (see that work also for a definition of kinetic terms such as, e.g., "apparent" charge separation lifetime, "effective" charge separation rate constant, etc.). Entirely on the basis of a comparison with fluorescence kinetic data from the literature, we furthermore proposed the hypothesis that charge separation from the first RP is in fact reversible, which should give rise to noticeable charge recombination fluorescence.[7]

Although fully compatible with the reported transient absorption data, the hypothesis of a charge recombination fluorescence was not actually proven unequivocally by our transient absorption data. We indicated that this hypothesis needed verification by independent fluorescence kinetics studies on the same system.[7] We have now measured the fluorescence kinetics on the same w.t. samples of *C. reinhardtii* as used previously for the transient absorption study (with open RC, i.e., reduced P700) in order to test the charge recombination hypothesis. The rationale behind this study is that (i) the fluorescence kinetics are very sensitive to the charge separation and recombination rate constants and (ii) fluorescence kinetics should allow us to

* To whom correspondence should be addressed.

10.1021/jp046299f CCC: $30.25
Published on Web 03/08/2005

determine very accurately the effective charge separation and recombination rate constants and thus also the free energy gap between the first radical pair (RP1) and the excited reaction center (RC*) state(s). The present data offers clear proof of the charge recombination hypothesis which provides strong support for our new interpretation of energy and electron-transfer kinetics and the mechanisms proposed earlier.[7]

Materials and Methods

Samples. PS I cores from the green algae *C. reinhardtii* have been isolated as reported previously.[7] For the measurements, the PS I complexes were diluted to an $OD_{676} = 0.068$/mm in 25 mM Tricine-NaOH (pH 7.5), 0.02% DM, 50 mM NaCl, 20 mM Na ascorbate, and 40 μM phenoxy-methosulfate (PMS) as redox mediator in order to keep the RCs in an open state. The measurements were performed at room temperature (22 °C) in a 1.5 mm path length flow cuvette through which the sample was pumped by applying a constant pressure of nitrogen gas in order to maintain a constant flow speed. We checked carefully that RCs were strictly open under our conditions (this condition was also rationalized by calculations based on the applied flow speeds, the laser intensity, repetition rate, and the optical density of the samples). Integrity of the sample was checked by absorption and steady-state fluorescence spectroscopy before and after the measurements. No changes in the spectra were observed.

Time-Resolved Fluorescence. Picosecond time-resolved fluorescence was measured by the single-photon-timing technique, using a synchronously pumped, cavity-dumped dye laser as described previously[8−10] with a repetition rate of 800 kHz and DCM as the laser dye. The optical pulses were in the range of 10−15 ps, and the overall system prompt response was typically 30−35 ps (fwhm). The energy of a single excitation pulse was low enough to excite less than 1 out of 10^4 PS I particles in the sample volume. The combination of pumping rate (about 2 mL/s), pulse energy, and repetition rate also ensured that only a negligible amount of PS I particles (in the order of <1%) received a second consecutive excitation from the laser. Data analysis has been performed initially by global lifetime analysis. Global target analysis was applied on the original 3D (intensity vs time and wavelength) fluorescence decay data for testing kinetic models and for determining the rate constants and species-associated spectra (SAS).[11] We recorded the data with a very high S/N ratio (peak counts up to 30 000) at most wavelengths. Under these conditions, the time resolution of the system is 1−2 ps.[8] This means that a component in that time range can still be determined in global target analysis with an accuracy of about 30%, if its relative amplitude is in the order of 30% or larger in at least part of the covered spectral range.

Definition of Kinetic Terms. Throughout this paper we will use the terms "lifetime" or "apparent lifetime" for the kinetic components that can be observed experimentally and for the corresponding lifetime parameters resulting from the solution of a kinetic model. One of the main confusions in this field stems from the incorrect use of terms such as "rate constants" or sometimes "rates" for the inverse of these lifetimes. The term "rate constant" is strictly reserved for the so-called "effective rate constants", which are rate constants for energy transfer or electron-transfer processes between compartments determined within a specific kinetic model (see ref 11 for all of these definitions). Likewise, the term "intrinsic rate constant" is reserved for the pair wise rate constants of energy transfer or electron transfer (i.e., for single step processes between neighboring pigments). With very few exceptions, both the "effective rate constants" as well as the "intrinsic rate constants" cannot be measured directly in a time-resolved experiment. Rather these parameters are only defined and can only be determined from the experimental kinetics (lifetimes, amplitudes, time-resolved spectra, etc.) within a specific kinetic model. Only in very rare cases, which will not be discussed here, may an experimentally accessible "lifetime" be identical to the inverse of either an "effective" or "intrinsic" rate constant. Following these simple rules will avoid most of the confusions that have plagued and continue to plague the interpretation of experimental data as well as the discussion and comparison of kinetic models in this field. Most of these definitions have been provided in the literature.[7,11]

Figure 1. Kinetic compartment model for energy and electron-transfer processes in PS I for *C. reinhardtii* as proposed based on femtosecond transient absorption data (taken from ref 7). Note the three radical pairs and the charge recombination process from the first radical pair to the RC excited state. Ant, antenna pools; RC, reaction center; RP1 to RP3, radical pairs; rate constants are given in units of ns^{-1}.

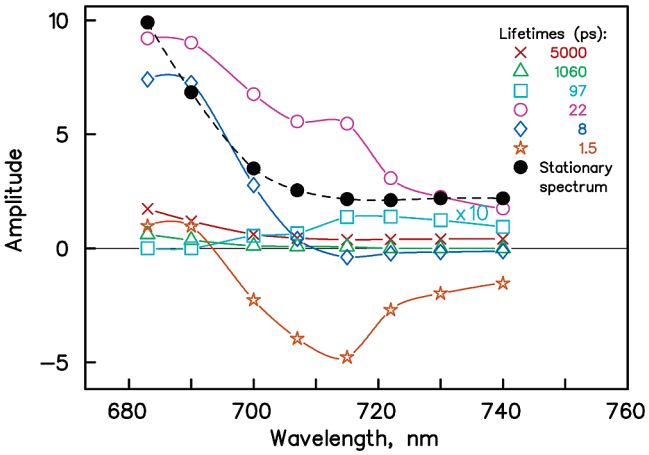

Figure 2. Stationary fluorescence spectrum (full black circles) and decay-associated spectra (DAS) and lifetimes of the fluorescence of PS I core particles of *C. reinhardtii* excited at 675 nm obtained by global analysis of the fluorescence decays. Note that the DAS amplitudes of the 97 ps component have been multiplied by a factor ×10 for clearer presentation.

Results and Discussion

An excitation wavelength of 675 nm has been used, i.e., close to the absorption maximum of the particles. Fluorescence kinetics have been detected at various wavelengths in the range 682−740 nm in intervals of 7−10 nm with a 5 nm bandwidth. The stationary fluorescence spectrum and the DAS resulting from the global lifetime analysis are shown in Figure 2. As discussed previously,[7] the samples contain a small (corresponding to 5−10% of absorption at 670−675 nm) amount of energetically uncoupled LHC I complex. This antenna complex gives rise to long-lived (ns) fluorescence which dominates the total fluorescence yield (cf. Figure 2).

Altogether six kinetic components were necessary to describe the fluorescence kinetics perfectly over the whole range of several nanoseconds (Figure 2). When using an abbreviated time range of 300−600 ps only, which is quite sufficient to resolve all lifetime components associated with the intact PS I cores, the two long-lived nanosecond components could be combined into one, and consequently, five components were sufficient to analyze the data. This shorter range and reduced component number was used in most subsequent analyses. The dominant amplitude components are 1.5, 8, and 22 ps. The other three lifetimes have much smaller amplitudes. The fastest three components with large amplitudes clearly have to be assigned to intact PS I core particles. A 97 ps component has an extremely small, but still significant amplitude in the red part of the spectrum (note that in Figure 2 the amplitude of this component has been multiplied by a factor of 10), whereas the two components in the nanosecond range (for a long analysis range) with lifetimes of 1 and 5 ns have similar spectra peaking at a wavelength shorter than 682 nm. The combined amplitude of the two nanosecond components is about 10% at 682 nm. These nanosecond components can be assigned to the energetically uncoupled LHC I complexes in the sample. The assignment of the very small 97 ps component is not clear at present, and we omit it in the further analysis and interpretation. Since several long-lived lifetime components contribute significantly to the overall fluorescence yield (in particular the LHC I fluorescence), the measured stationary fluorescence spectrum (cf. Figure 2) does not reflect the fluorescence spectrum of the PS I core particles but resembles more the spectrum of the uncoupled antenna complexes. We can however calculate the hypothetical stationary fluorescence spectrum of the intact PS I cores by summing the contributions of the three short-lived components only. This calculated spectrum (not given) is very close to the spectrum of the 22 ps component (cf. Figure 2) and dominates the fluorescence of the intact core.

The fastest lifetime component, ≈1.5 ps, is an energy transfer component which has a small positive contribution at short wavelength and a dominant negative contribution above 690 nm (Figure 2). It should be noted that this component is at the limit of the time resolution of our apparatus, and we therefore have to assume a fairly large error of about 30% in both lifetime and amplitude. Due to its large amplitude, we can however still resolve such a fast component in global analysis where more stringent restrictions apply than in free running single lifetime analysis.[11,12] In the transient absorption data, we found 600−900 fs and ≈ 2 ps energy transfer components, the former with the dominant amplitude. We thus expect that the 1.5 ps fluorescence component found here reflects mainly the ≈ 2 ps transient absorption component, with some unresolved mixing-in of the shorter-lived subpicosecond energy transfer component. The wavelength range of positive and negative amplitudes and the zero-crossing wavelengths for this component are in good agreement with the expectations based on the corresponding transient absorption components whose negative lobe extends up to about 715 nm (see Figure 3A of ref 7). We estimate that the maximum of the fluorescence DAS spectra should be red-shifted by 3−4 nm, i.e., about half the Stokes shift of the Chl molecules, relative to the corresponding maxima in the transient absorption spectra since the fluorescence spectra lack the shorter-wavelength absorption bleaching contribution and reflect only the stimulated emission part of the transient absorption signal. We should note that a similar component, both in spectrum and lifetime (0.7−1 ps range) has been observed in the fluorescence kinetics of *Synechocystis* PS I monomeric cores[13] which was performed with higher time resolution than our measurements reported here.

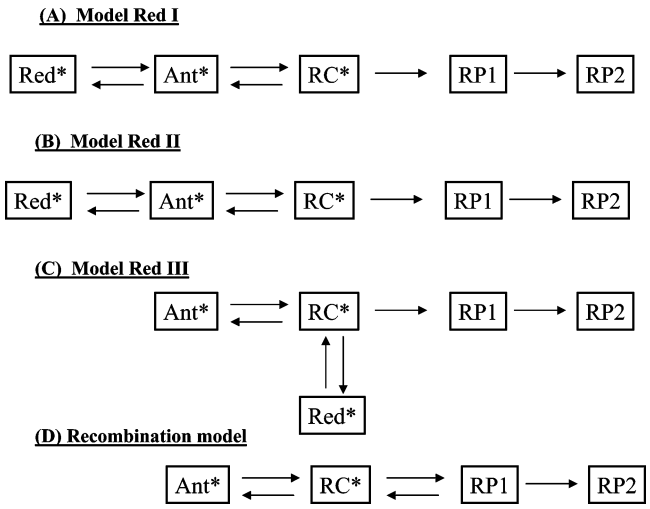

Figure 3. Kinetic compartment models as tested in this work. (A) and (B) represent "red antenna" models where the red pigment pool (Red) is connected to the core antenna (Ant) (Note that Scheme B is formally the same as Scheme A; as compared to Scheme A it has been analyzed by imposing some restrictions in the starting conditions however). RP1 and RP2 represent the first two radical pairs in the electron-transfer pathway and RC the reaction center. (C) represents a "red antenna" model (red III) where the red pigment pool is connected to the RC. Model (D) is the charge recombination model which does not contain a red antenna pool and the first electron-transfer step is reversible, leading back to the RC* reaction center excited state.

The 8 ps component (Figure 2) shows large positive amplitude up to 700 nm and a small but significant negative amplitude above 710 nm. The small negative amplitude contribution indicates that this component involves mainly energy trapping by charge separation with perhaps some minor mixing-in of energy transfer. It is interesting to compare this component to the spectrum (large positive and small negative amplitude at longer wavelengths) of a 5.4 ps component which was observed for short excitation wavelengths (up to 660 nm) in the fluorescence of monomeric *Synechocystis* PS I cores.[13] We assume that the 5.4 ps component observed by those authors may in fact arise from a dominant 8−9 ps contribution (a strong 9.4 ps component was indeed resolved for 702 nm excitation in that work) and some unresolved lifetime contribution of about 2−3 ps. The 22 ps component is all positive in amplitude with a maximum near 682 nm and a pronounced shoulder near 712 nm. Again this fluorescence component is reminiscent of a similarly shaped component (lifetime of also 22 ps) in the fluorescence of monomeric *Synechocystis* PS I cores.[13]

For *C. reinhardtii* PS I cores, little high resolution kinetic data with clearly defined measurement conditions with regard to the RC redox state exist in the literature. The data of Melkozernov et al.[14] do show the presence of a large 20−25 ps fluorescence component. However, the measurements did not resolve any faster components which makes an overall comparison difficult. The best time-resolved fluorescence lifetime study for *C. reinhardtii* core PS I has been performed by fluorescence up-conversion[15] and showed the presence of a 5.5 ps fluorescence component. However, neither in our transient absorption data nor in the present fluorescence kinetics is such a 5.5 ps component present. Rather, in transient absorption, the energy transfer components were about 0.8 and 2 ps.[7] Thus, it is very likely that the 5.5 ps component of Du et al.[15] represents a mixture of the 1−2 ps energy transfer component and the

7−9 ps trapping component found in our transient absorption study. Lifetime components of 3.8 and 9.8 ps have also been resolved in a combined up-conversion and streak camera fluorescence study.[16] However, the necessity to excite at short wavelengths, far away from the Chl Q_y absorption maximum, introduced additional short-lived components into the kinetics which disturbed the kinetic analysis. A ≈10 ps component with similar spectral shape as found here for the 8 ps component has been resolved also for trimeric *Synechococcus* PS I, but could not be assigned within a detailed kinetic model.[13]

Kinetic Modeling. We now go on to perform global target analysis on the fluorescence kinetics to calculate rate constants and SAS within various kinetic compartment models. Note that all of the target analyses have been performed directly on the original 3D fluorescence data and not on the results of the global lifetime analysis.[11]

With three resolved lifetime components belonging to the intact PS I cores, we can analyze a kinetic model involving a maximum of three fluorescent (quasi)-species. Under such conditions, one is able to determine a maximum of five independent rate constants in the fits.[11] At least one of the fluorescent species taken into account will have to be the (equilibrated) antenna excited state. We know from our previous transient absorption study that, in principle, two antenna components (or compartments) should be resolved. However, since the fast energy transfer component with subpicosecond lifetime is not resolved in our fluorescence study at this stage, we have to resort here to somewhat simpler models by combining the two antenna pools into a single antenna pool only. The implications of this model simplification as compared to the analysis of the femtosecond transient absorption data will be discussed below. It can be shown however that the consequences with respect to the determination of the charge separation and charge recombination rate constants, which are our prime interest in the present work, are in fact minor.

A variety of kinetic models have been tested which represent three formally different kinetic models and mechanisms. These are shown in Figure 3A−D. Figure 3, parts A and B, represents the so-called "red antenna model" (models red I and red II). This is essentially the traditional scheme which has been extensively used in the literature for analyzing PS I fluorescence kinetic data[17−21] (see, e.g., ref 22 for a review). There is one important difference present in all our kinetic models as compared to all previously used models (see, e.g., the discussions in refs 7 and 21). We explicitly assign a fluorescent state to the equilibrated excited reaction center state RC* from which charge separation occurs. In the older schemes describing fluorescence kinetics, the trapping was assumed to occur directly from the antenna by an undefined and nonfluorescent "trap state", which was implicitly assumed to be some kind of a combined RC*/RP1 state (cf., e.g., ref 22 and the extensive discussion in our previous work ref 7). Thus, in fact the RC* state was considered to be nonfluorescent. The (implicit or explicit) assumption to justify this model was that either the charge separation from the RC* state is ultrafast, which would lead to very low fluorescence from the reaction center, and/or the intermediate population of excited RC was assumed to be very small, due to a diffusion-limited or "transfer-to-the-trap-limited" kinetics. However, on closer inspection, these assumptions cannot be upheld. First, the fluorescence transition moment of the RC pigments is expected to be at least as large as for individual antenna Chls, if not larger due to the formation of some superfluorescent states caused by medium to strong exciton coupling among the RC Chls. Second, the effective charge separation rate constant from the energetically equilibrated RC* (6 Chls) cannot be much larger than $(2\ \text{ps})^{-1}$, even if we assume a subpicosecond intrinsic electron transfer rate constant. We have recently shown that the "apparent" antenna trapping lifetime for *C. reinhardtii* PS I cores is in the range 7−9 ps and that the excited RC should be populated to an appreciable amount, i.e., up to about 25% relative population.[7] Previously Savikhin et al. had also argued on different grounds in the same direction.[23] Comparison with the apparent charge separation lifetime from the equilibrated PS II RC* is also in order here, which is known to be in the range of 3−7 ps[24−27] in intact systems and similarly long in its main components for isolated PS II RCs.[28,29] For this reason, all our tested models have to take into account explicitly the fluorescence contribution from the excited RC which may be of similar intensity as the antenna fluorescence.

Global Target Analysis. The results of global target analysis for the various models (cf. Figure 3A−D) are given in Figure 4A−D (rate constants, lifetimes, eigenvectors, and the time dependence of populations), whereas Figure 5A−D shows the corresponding species-associated spectra SAS for the respective models. In all cases, it has been assumed that excitation at 675 nm is absorbed with 98% or higher probability (this does not include the absorption of the separate LHC I contamination) in the core antenna (Ant) and that the "red antenna" state (red) and/or the RC receive negligible excitation. Fitting of all these models by global target analysis occurred directly on the 3D surfaces of fluorescence intensity vs wavelength and time.[11] As pointed out above, model 3A (model red I) is, except for the explicit addition of the fluorescent state for the RC*, the traditional PS I kinetic model that assumes the presence of a "red antenna" state being present somewhere in the core antenna (Note that we do not show here any models that do not take into account explicitly fluorescence from the RC* state since they did not give any reasonable fitting results at all.) Formally, model 3B (model red II) is identical to 3A. However we have forced the system into a second minimum which yields a faster charge separation rate constant by applying special starting parameters for the fit. This has been tried in order to test whether the fluorescence kinetics data would perhaps also be consistent with the "red antenna" model but using the much faster apparent charge separation or trapping lifetime that had been predicted by our transient absorption study.[7] In model 3C, the "red antenna" state is attached not to the core antenna, as is usually assumed, but to the RC directly. However, the red antenna is not part of the RC itself in this model. In all models 3A−C, the charge separation to the first radical pair is assumed to be irreversible, in keeping with the previously assumed irreversibility of the charge separation in PS I (see ref 7 and also the review of Brettel and Leibl[1] for an extensive discussion on that topic). Finally, model 3D ("recombination model") essentially represents the new model for energy transfer and charge separation that we proposed earlier based on our transient absorption study.[7] It contains no "red antenna" state in the core, and the charge separation process is reversible, leading back to the excited RC. With respect to our previous full model based on the transient absorption data, this model lacks only the ultrafast subpicosecond antenna equilibration component which is not resolved in our present fluorescence data. The somewhat simplified model used here had also been tested previously (Figure 4 of ref 7) and was found to result in a very good, albeit not perfect, fit to the transient absorption data. However, all of the essential elements of the mechanism of the new "recombination model" are contained in this model.

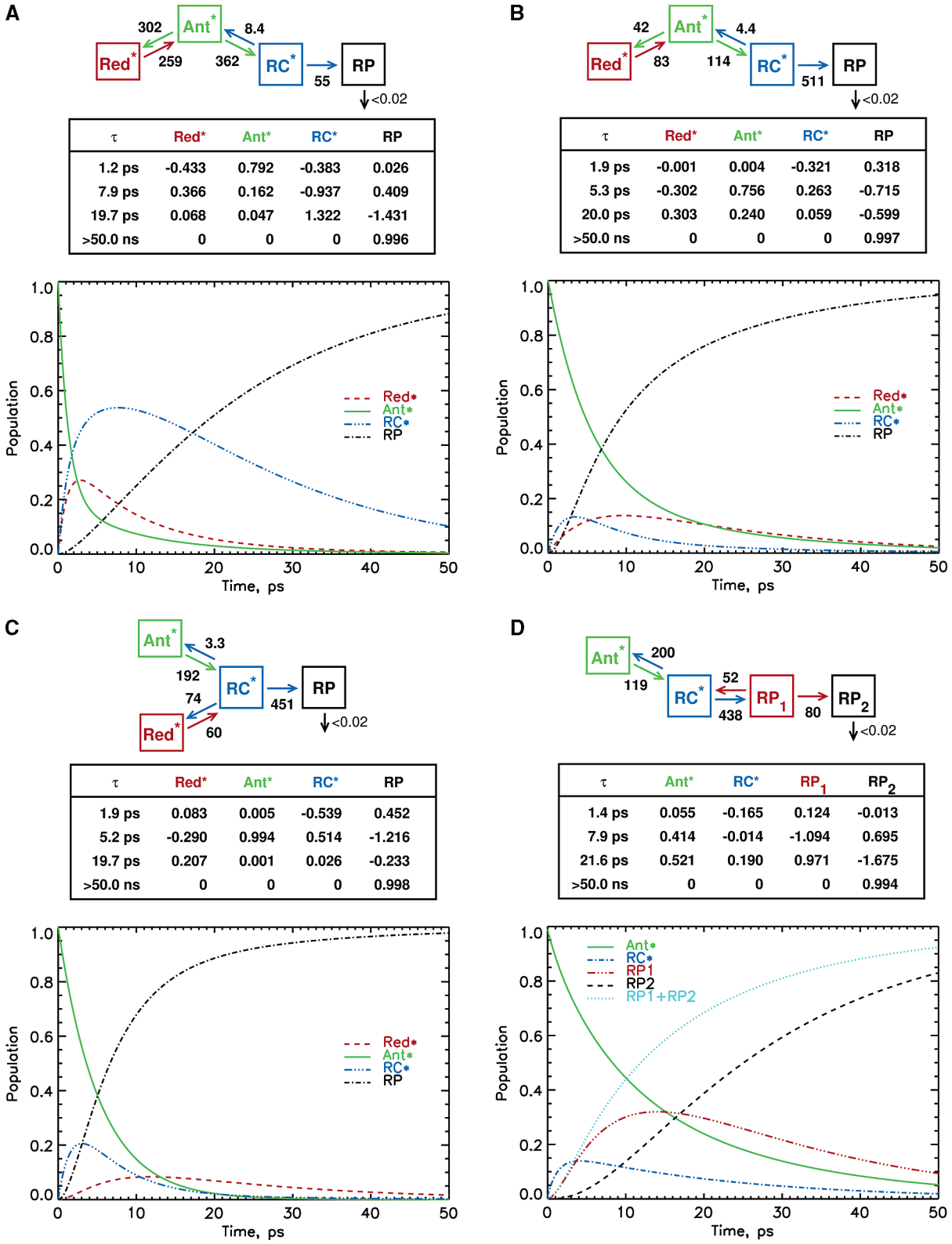

Figure 4. Compartment model with rate constants (ns^{-1}) (top), lifetimes and eigenvectors (center), and time dependence of relative populations (bottom) for the kinetic models tested (cf. Figure 2). (A) Model "red I", (B) model "red II", (C) model "red III", (D) "recombination model".

We now discuss the results of fitting these various kinetic models to the fluorescence kinetics. Formally, the fitting quality within the global target analysis is about equally good for all of the models. This is not very surprising, since all of the models yield very similar sets of lifetimes. Thus, from a formal fit quality criterion for lifetime fitting alone, no distinction is possible between these models. It is however not sufficient for a complex system such as this one to check simply for a good formal fit. Rather the results must be examined for the physical consistency of the SAS, the rate constants, and the spectral assignments. A close examination reveals that there exist very important differences in the rate constants and SAS associated with these different models. We will in the following discuss these differences in detail and will show that models 3A−C, i.e., all of the "red antenna" models, predict either physically unreasonable spectra, unreasonable rate constants, or both.

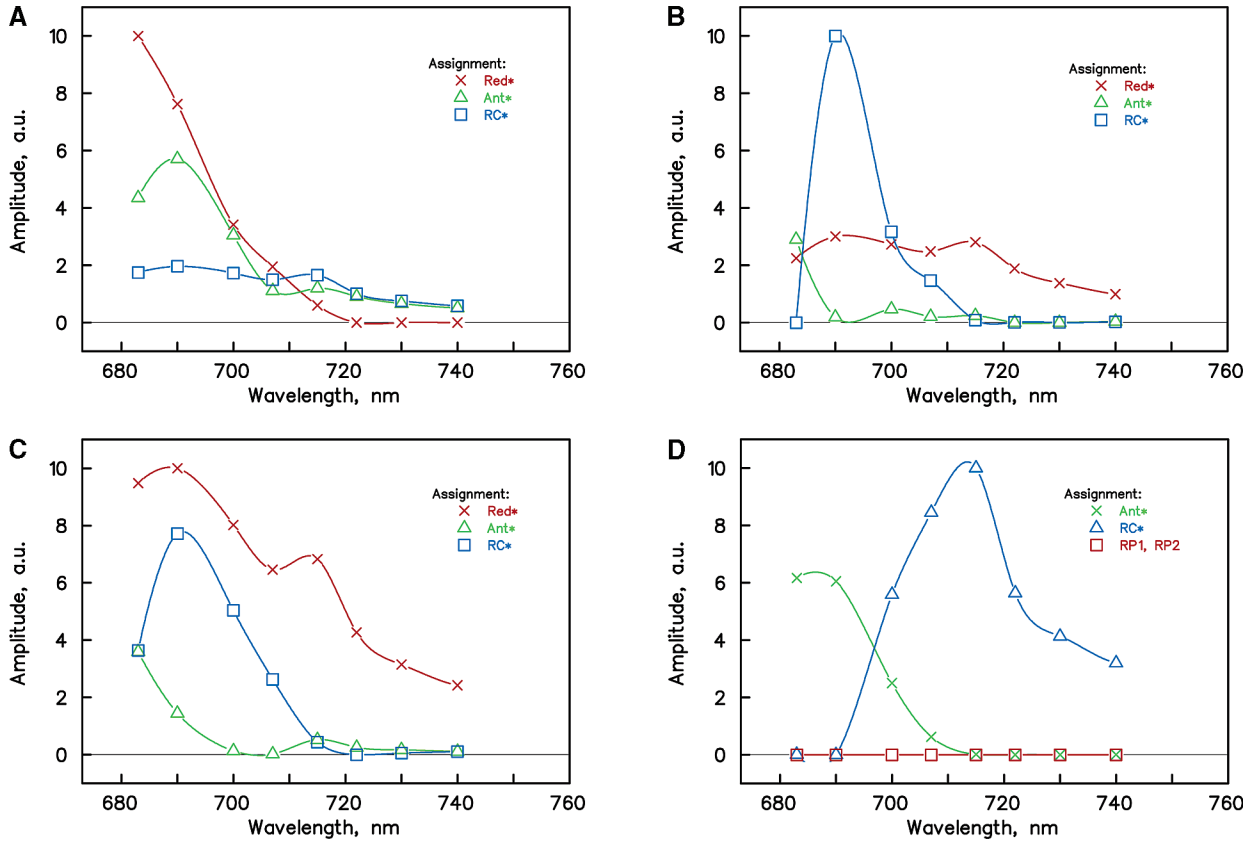

Figure 5. Species-associated spectra (SAS) obtained from global target analysis of the fluorescence data for all of the models tested in this work (cf. Figure 2). Ant*, antenna spectrum; Red*, red antenna fluorescence spectrum; RC*, reaction center fluorescence spectrum; RP1 and RP2, radical pair fluorescence spectra (set to zero due to the RP being nonfluorescent). (A) Model "red I", (B) model "red II", (C) model "red III", (D) "recombination model".

Model 3A (red I) yields lifetimes of 1.2, ≈8, and ≈20 ps (cf. Figure 4A). This is in good agreement with the lifetimes obtained from the transient absorption data[7] with the exception of the ultrafast 600−900 fs component (see discussion above). Inspection of the eigenvectors (Figure 4A) shows that the trapping (congruent with formation of radical pair RP1) occurs exclusively with the ≈20 ps lifetime component, in agreement with the earlier analogous kinetic models (see the review in ref 22). This is much slower than the apparent RP1 rise time of 7−9 ps required by our transient absorption data. Note that in this model the excited RC reaches an extremely high maximal relative population of about 55%, by far the highest of all the tested models, which requires a very high contribution of RC* fluorescence to the total fluorescence. This fact alone invalidates previous applications of equivalent models which entirely ignored the RC* fluorescence.[21] As can be seen from inspection of the eigenvectors in this model (Figure 4A), the hypothetical "red antenna" state is populated with the 1.2 ps kinetics and decays with the ≈8 ps lifetime. The RC excited state is populated in a biexponential kinetics with the 1.2 and ≈8 ps components and decays with the ≈20 ps component, in keeping with the ≈20 ps "apparent lifetime" for formation of the RP1 in this model. Inspection of all the rate constants shows however that the ratio of effective forward to back energy transfer rate constants between antenna and RC, which is ≈43, is physically untenable. Assuming an energy difference of 400 cm^{-1} between the average antenna excited state (not taking into account the hypothetical "red antenna" state) and the average RC excited state (this energy difference is typically used for PS I using antenna energy corresponding to 680 nm and RC energy corresponding to 700 nm transitions), and assuming, furthermore, 90 antenna Chls and 6 RC Chls, that ratio should be about 0.5 based on the Boltzmann equation. The transient absorption data[7] suggest that the average energy difference between antenna and RC excited states might in fact be even smaller in the core PS I of *C. reinhardtii*, i.e., only about 300 cm^{-1} (the energies used for this estimation are those from the bleaching maxima of antenna and equilibrated RC* in the transient absorption data).[7] A 300 cm^{-1} energy difference translates to an even smaller ratio of the effective rate constants for forward to backward transfer than 0.5 (i.e., about 0.3−0.4). Inspection of the SAS (Figure 5A) also excludes this model, since in fact the assumed "red antenna" state is not a "red Chl" but is predicted to have an emission maximum even shorter than the core antenna, i.e., below 680 nm. In addition, the RC* emission spectrum is predicted to have two maxima, one at around 690 nm and a second maximum of equal magnitude at about 712 nm. Thus, both the predicted "red antenna" fluorescence and the RC* fluorescence spectra are physically highly unreasonable and not in agreement with the implicit assumptions of the model. Furthermore the ratio of the effective forward/backward energy transfer rate constants is physically entirely unreasonable. Thus, we can safely exclude this model on the basis of the fluorescence data alone. It is however also inconsistent with the transient absorption data, mainly due to the much too slow charge separation/radical pair formation (effective rate constant 55 ns^{-1}) that it predicts.

For fitting model "red II" (Figures 4B and 5B), we tested whether a second minimum on the global fitting surface can be found by forcing a faster effective charge separation rate constant. This is indeed possible since this model also gives a formally good fit. After starting the fitting procedure with a much higher charge separation rate constant and some other modified starting parameters as compared to model 3A, the

fitting procedure found a minimum with a fit quality similar to that for model 3A. Once a solution had been found, it was thus not necessary to keep the charge separation rate constant fixed to the high value set at the start. The optimal value for the effective charge separation rate constant is now 511 ns^{-1}. We consider this value still to be within an acceptable range based on our transient absorption data, though at the upper limit. The ratio of the forward/backward rate constant of energy transfer antenna/RC is about 26 in this case. This value is still more than an order of magnitude off the expected Boltzmann ratio of 0.3−0.5. The apparent kinetics for radical pair formation are now faster on average, with biexponential kinetics of 5.3 and 20 ps. The faster lifetime component has a somewhat larger contribution (see eigenvectors in Figure 4B). The formal "red antenna" state is populated with the 5.3 ps lifetime component and decays with the 20 ps lifetime component. The RC* population only reaches about 15% in the maximum. Formally, the overall predications of this model seem to be in better agreement with the previous "red antenna" models of the PS I kinetics, which assumed a slow decay of the "red antenna" state and a "nonfluorescent" RC. However, inspection of the predicted SAS in Figure 5B clearly leads us to rule out this model as well. The RC* fluorescence maximum is predicted at 690 nm with a strong band, about two to three times more intense than the spectra of the "red antenna" and the main antenna spectrum (Ant*). Yet the hypothetical "red antenna" state now looks such as the RC* emission spectrum in model 3A (Figure 5A), i.e., two peaks at 690 and 712 nm, which is very unreasonable for the assumed "red antenna" state. The core antenna does not possess a physically reasonable fluorescence spectrum either, showing a maximum below 680 nm (not clearly defined in our data since we could only start to measure fluorescence at 682 nm). The predicted charge separation rate constant in this model is again not in agreement with the findings of the transient absorption measurements. Thus, we can safely exclude this model since it also fails to provide a physically reasonable description of the energy transfer and charge separation processes in these PS I particles.

In model "red III" (Figure 3C, cf. Figures 4C and 5C), the hypothetical "red antenna" is connected in terms of the dominant energy transfer steps not to the core antenna but to the RC, thus implying that the "red antenna" is sitting close to the RC, but not being part of the RC. The predicted charge separation rate constant in this case is quite high (451 ns^{-1}), and the overall formation of radical pair is biexponential, showing lifetimes of 5.2 ps (dominant component) and 19.7 ps (about 20% contribution). Population of the formal "red state" occurs with the 5.2 ps lifetime, and it decays with the 19.7 ps lifetime. The RC* population rises with a lifetime of 1.9 ps, i.e., close to the fast rise observed in the transient absorption data. However the antenna/RC energy transfer rate constants show a ratio of 42, again far away from any physically reasonable value. The maximal RC* population reaches about 20%. The predicted SAS fluorescence spectra (Figure 5C) are similar to those of model 3B (Figure 5B), although with different relative amplitudes. Major problems in this model are the RC* emission spectrum with a maximum at 690 nm and even more so the fact that the formal "red antenna" state is again not a "red antenna", but shows a maximum at 690 nm, i.e., at only slightly longer wavelength than the core antenna and at the same position as the maximum of the RC* fluorescence. A second smaller maximum at 712 nm is however apparent. The overall judgment of the predictions of this model and in particular the comparison with the transient absorption data both in terms of the expected spectra, the kinetics of radical pair formation,[7] and the ratio of forward/backward energy transfer rate constants again lead us to conclude that this model does not result in physically reasonable predications and must thus be excluded.

Figures 3D and 4D show the "recombination model" that we had already proposed in our previous study.[7] This model predicts lifetimes of 1.4, 7.9, and 21.6 ps for the fluorescence kinetics. Please note that this model has fewer free parameters in the fit than all of the previously discussed models 3A−C since there is no "red antenna" state present and the fluorescence of the radical pairs can be set to zero. It contains the same number of free rate constants (a total of 5) but only two fluorescence spectra to be determined as free parameters of the fit. The fact that with this much more restricted parameter set we get the same good fit quality as for the other models already provides a first positive hint toward this model. Inspection of the eigenvectors in Figure 4D shows that the formation of RP1 occurs exclusively with the ≈ 8 ps lifetime and formation of RP2 with the 21.6 ps component, in excellent agreement with the transient absorption data.[7] Antenna/RC equilibration occurs with the 1.4 ps lifetime component, again in good agreement with the average lifetime of the antenna/RC equilibration from the transient absorption data. The ratio of the effective antenna/RC forward to backward rate constants is now only 0.6, i.e., drastically smaller than in the models 3A−C (see above). The predicted maximal RC* population in this model is about 16%, i.e., somewhat smaller than the ≈25% observed in the transient absorption data. This is in part attributable to the lack of resolving the ultrafast energy equilibration component[7] which leads to some underestimation of the average population of RC*. It is important to note that the apparent lifetime for charge separation (which is identical to the rise time of the RP1, cf. the eigenvector matrix in Figure 5D) of 7.9 ps is very well defined in the fluorescence kinetics. The effective charge separation rate constant is 438 ns^{-1}, which is about 40% larger than the corresponding rate constant determined from the transient absorption data. This increase can be explained only in part by the unresolved ultrafast antenna equilibration component in our fluorescence data. Rather, it is mainly a consequence of the substantially larger effective charge recombination rate constant of 52 ns^{-1} that is predicted from the fluorescence data. Its value is about twice as high as that chosen to fit the transient absorption data. We remind the reader however that we had pointed out in that work that the charge recombination rate constant had been determined imprecisely in the fits to our transient absorption data.[7] The value of 25 ns^{-1} used there was merely the middle range of the upper and lower limits that were still compatible with those data. The charge separation and charge recombination rate constants are clearly much better defined in the present fluorescence kinetics analysis, and we estimate the error to be only about 10−15%. We note again that a precise determination of the effective charge separation and charge recombination rate constants is at the focus of the present work. The rate constant of secondary electron transfer from RP1 to RP2 in this model is in excellent agreement between the two sets of measurements. This is a direct consequence of the fact that the ≈8 and 22 ps components are very well determined in our fluorescence data, both in terms of the lifetimes and in terms of the amplitudes. Above all, analysis of the fluorescence kinetics is simpler than the transient absorption kinetics, since the radical pairs do not contribute directly to fluorescence.

For the "recombination model" the agreement in both rate constants and overall kinetics of the fluorescence data with the transient absorption data, within the limitations due to the

experimental resolution discussed above, is very good. Another important point in support of this model is however the fluorescence SAS shown in Figure 5D. The maximum of the core antenna fluorescence spectrum is at 687 nm, in very good agreement with expectations. The spectral shape is very reasonable showing basically a single, roughly Gaussian, band with a half width of about 25 nm. The RC fluorescence spectrum has an about 50% higher amplitude than the antenna SAS (note that the area under the fluorescence spectra should be proportional to the radiative rates of the emitting states[11,12]). The maximum is at about 712 nm, and there is a shoulder at about 700 nm and a second more pronounced shoulder at 730 nm. We consider this to be a very reasonable spectrum for the equilibrated RC* state, originating from the ensemble of six exciton states of the 6 RC Chls, which are equilibrating their excitation energy with a typical 150 fs lifetime.[7] Our data implies that the RC exciton states with the maximal oscillator strength should be located in the range 695−705 nm, which is also suggested by exciton calculations.[30] Thus, the predicted spectra are in good agreement with both the expected antenna and the RC* properties. We conclude that the "recombination model" is the only one of all of the models tested which predicts physically reasonable rate constants and spectra and furthermore provides full agreement with the transient absorption data.

Conclusions

Depending on our assumptions of how many exciton states of the RC* state are involved directly in the charge recombination with the first RP, we can estimate from the ratio of the forward and backward electron-transfer rate constants, free energy differences of about 580 cm^{-1} (for the assumption of 2 exciton states) to 800 cm^{-1} (assuming a contribution of all 6 RC exciton states) between the RP1 state and the average RC* state. Thus the RP1, despite its substantial contribution of charge recombination fluorescence to the total fluorescence yield and kinetics, is still a relatively deep trap state, with an energy difference to the excited state of 2−4 times kT. This also explains the overall high rate of forward reaction in the PS I RC.

Properties of the RC. According to the rate constants given in Figure 4D, the initial trapping time from the equilibrated excited state of a hypothetical "isolated RC" particle, comprising only the 6 RC Chls as pigments and the electron acceptor chain, would be expected to be about 2 ps. The "apparent charge separation lifetime", equivalent to the rise time of the first radical pair (Figure 4D) of ≈8 ps is due to the "antenna effect"[31,32] which lengthens the apparent charge separation time vs the apparent charge separation lifetime of the hypothetical isolated RC, devoid of antenna, by a factor of about 4. The apparent trapping time of the hypothetically isolated PS I RC of ≈2 ps in our "recombination model" is much shorter than the corresponding lifetime of about 9−10 ps assigned in studies of P700 enriched PS I particles.[5,6] We note that these authors, upon direct RC excitation, also attributed a ≈0.8 ps component to charge separation. We concur that this fast charge separation rate may be possible upon direct excitation of the electron donor state, although the ultrafast 150 fs exciton equilibration time in the RC makes it unlikely that charge separation from the directly excited electron donor can be observed experimentally. However, their lifetime of the equilibrated RC* state of 9−10 ps is too slow by a factor of 5 compared to our data. This discrepancy means either that the assignment of that component is incorrect (note that charge recombination has been ignored in their analysis), or that the P700 enriched RCs prepared by the ether extraction method are not intact any more. Unless the charge separation were to occur from one of the high energy Chl pigments it would be hard to understand why the charge separation from the energetically equilibrated RC should take a factor of 10 longer than for the directly excited "P700*" state in intact PS I cores. We note here in passing that in our view it is not known what the "P700*" state actually means in terms of the excitation state(s). The term "P700" is essentially only defined in a meaningful manner for the oxidized form of the RC, i.e., as $P700^+$.

The data presented here fully support the charge recombination hypothesis introduced initially in our recent PS I work[7] as the only acceptable kinetic model. All of the other models tested here can be safely excluded on various grounds. This conclusion is not compromised in any way by the fact that the time resolution of our fluorescence apparatus is at the limit for resolving the antenna equilibration time and thus causes a large error margin for this component in the order of 30−40%. Rather the differences between the models, in particular the differences in the ratio of forward/backward energy transfer rate constants between antenna and RC and also the difference in the SADS, are so dramatic for the various models − within the same set of lifetimes and DAS − that the mechanistic differences and the following conclusions cannot be altered dramatically by a more precise measurement of the fastest component.

The previously proposed "charge recombination" model is clearly confirmed by the critical test of the fluorescence kinetics. This has various important consequences. The average energy equilibration lifetime antenna/RC is about 1 ps in the recombination model (even faster if the high-resolution transient absorption data are taken as a basis) vs the 4−5 ps equilibration lifetime within model "red I" which formally represents the model proposed earlier by many authors (see, e.g., ref 21 and references therein). In fact previous modeling resulting in the proposal of a "transfer-to-the-trap-limited model" has assumed that the 20−24 ps component is the apparent energy transfer rate-limited lifetime of core antenna trapping (Note that this apparent lifetime in the "transfer-to-the-trap-limited model" is identical with the apparent lifetime of the formation of the first radical pair), which would translate into an even slower antenna/RC equilibration time than the 4−5 ps which we obtain within such a model.[21,22] In contrast, within the "recombination model" the apparent core trapping lifetime (identical with the apparent lifetime for the formation of the first radical pair RP1) is about 8 ps, i.e., by a factor of nearly 3 shorter than in the "transfer-to-the-trap-limited model". Thus within the new model trapping of excitation energy from the excited core is trap-limited and not diffusion-limited.

Another important consequence of our model is the absence of a "red antenna" state in the PS I core. Note that intact *C. reinhardtii* PS I as well as all higher plant PS I carries peripheral LHC I light-harvesting complexes which do possess "red antenna" states.[33−36] It follows from our analysis that the red-shifted fluorescence in *C. reinhardtii* is entirely due to the RC* fluorescence at room temperature (RT) and consequently any "red states" present in this PS I core are located in the reaction center itself. In contrast all cyanobacterial PS I particles have been found to contain a so-called C708 pigment, located outside the RC in the core antenna, which fluoresces at around 708−715 nm at room temperature and can be observed in absorption and hole-burning spectra to absorb at about 708 nm at low temperatures and about 702 nm at RT.[21,22,37]

References and Notes

(1) Brettel, K.; Leibl, W. *Biochim. Biophys. Acta* **2001**, *1507*, 100−114.

(2) Jordan, P.; Fromme, P.; Witt, H. T.; Klukas, O.; Saenger, W.; Krau*β*, N. *Nature* **2001**, *411*, 909−917.

(3) Krau*β*, N.; Schubert, W.-D.; Klukas, O.; Fromme, P.; Witt, H. T.; Saenger, W. *Nat. Struct. Biol.* **1996**, *3*, 965−973.

(4) Ben-Shem, A.; Frolow, F.; Nelson, N. *Nature* **2003**, *426*, 630−635.

(5) Kumazaki, S.; Ikegami, I.; Furusawa, H.; Yoshihara, K. *J. Phys. Chem. A* **2003**, *107*, 3228−3235.

(6) Kumazaki, S.; Ikegami, I.; Furusawa, H.; Yasuda, S.; Yoshihara, K. *J. Phys. Chem. B* **2001**, *105*, 1093−1099.

(7) Müller, M. G.; Niklas, J.; Lubitz, W.; Holzwarth, A. R. *Biophys. J.* **2003**, *85*, 3899−3922.

(8) Müller, M. G.; Griebenow, K.; Holzwarth, A. R. *Chem. Phys. Lett.* **1992**, *199*, 465−469.

(9) Croce, R.; Dorra, D.; Holzwarth, A. R.; Jennings, R. C. *Biochemistry* **2000**, *39*, 6341−6348.

(10) Wendler, J.; Holzwarth, A. R. *Biophys. J.* **1987**, *52*, 717−728.

(11) Holzwarth A. R. *Biophysical Techniques in Photosynthesis. Advances in Photosynthesis Research*; Kluwer Academic Publishers: Dordrecht, The Netherlands, 1996; pp 75−92.

(12) Holzwarth A. R. *Methods in Enzymology. Vol. 246 Biochemical Spectroscopy*; Academic Press: San Diego, 1995; pp 334−362.

(13) Gobets, B.; van Stokkum, I. H. M.; van Mourik, F.; Dekker, J. P.; van Grondelle, R. *Biophys. J.* **2003**, *85*, 3883−3898.

(14) Melkozernov, A. N.; Su, H.; Webber, A. N.; Blankenship, R. E. *Photosynth. Res.* **1998**, *56*, 197−207.

(15) Du, M.; Xie, X. L.; Jia, Y. W.; Mets, L.; Fleming, G. R. *Chem. Phys. Lett.* **1993**, *201*, 535−542.

(16) Kennis, J. T. M.; Gobets, B.; van Stokkum, I. H. M.; Dekker: J. P.; van Grondelle, R.; Fleming, G. R. *J. Phys. Chem. B* **2001**, *105*, 4485−4494.

(17) Holzwarth, A. R.; Schatz, G. H.; Brock, H.; Bittersmann, E. *Biophys. J.* **1993**, *64*, 1813−1826.

(18) Turconi, S.; Kruip, J.; Schweitzer, G.; Rögner, M.; Holzwarth, A. R. *Photosynth. Res.* **1996**, *49*, 263−268.

(19) Turconi, S.; Schweitzer, G.; Holzwarth, A. R. *Photochem. Photobiol.* **1993**, *57*, 113−119.

(20) Karapetyan, N. V.; Dorra, D.; Schweitzer, G.; Bezsmertnaya, I. N.; Holzwarth, A. R. *Biochemistry* **1997**, *36*, 13830−13837.

(21) Gobets, B.; van Stokkum, I. H. M.; Rögner, M.; Kruip, J.; Schlodder, E.; Karapetyan, N. V.; Dekker, J. P.; van Grondelle, R. *Biophys. J.* **2001**, *81*, 407−424.

(22) Gobets, B.; van Grondelle, R. *Biochim. Biophys. Acta* **2001**, *1507*, 80−99.

(23) Savikhin, S.; Xu, W.; Chitnis, P. R.; Struve, W. S. *Biophys. J.* **2000**, *79*, 1573−1586.

(24) Roelofs, T. A.; Lee, C.-H.; Holzwarth, A. R. *Biophys. J.* **1992**, *61*, 1147−1163.

(25) Roelofs, T. A.; Gilbert, M.; Shuvalov, V. A.; Holzwarth, A. R. *Biochim. Biophys. Acta* **1991**, *1060*, 237−244.

(26) Konermann, L.; Gatzen, G.; Holzwarth, A. R. *J. Phys. Chem. B* **1997**, *101*, 2933−2944.

(27) Schelvis, J. P. M.; van Noort, P. I.; Aartsma, T. J.; van Gorkom, H. J. *Biochim. Biophys. Acta* **1994**, *1184*, 242−250.

(28) Müller, M. G.; Hucke, M.; Reus, M.; Holzwarth, A. R. *J. Phys. Chem.* **1996**, *100*, 9527−9536.

(29) Greenfield, S. R.; Seibert, M.; Govindjee; Wasielewski, M. R. *J. Phys. Chem. B* **1997**, *101*, 2251−2255.

(30) Gibasiewicz, K.; Ramesh, V. M.; Lin, S.; Redding, K.; Woodbury, N. W.; Webber, A. N. *Biophys. J.* **2003**, *85*, 2547−2559.

(31) Schatz, G. H.; Brock, H.; Holzwarth, A. R. *Biophys. J.* **1988**, *54*, 397−405.

(32) Schatz, G. H.; Brock, H.; Holzwarth, A. R. *Proc. Natl. Acad. Sci. U.S.A.* **1987**, *84*, 8414−8418.

(33) Melkozernov, A. N.; Schmid, V. H. R.; Lin, S.; Paulsen, H.; Blankenship, R. E. *J. Phys. Chem. B* **2002**, *106*, 4313−4317.

(34) Melkozernov, A. N. *Photosynt. Res.* **2001**, *70*, 129−153.

(35) Gobets, B.; Kennis, J. T. M.; Ihalainen, J. A.; Brazzoli, M.; Croce, R.; van Stokkum, L. H. M.; Bassi, R.; Dekker, J. P.; Van Amerongen, H.; Fleming, G. R.; van Grondelle, R. *J. Phys. Chem. B* **2001**, *105*, 10132−10139.

(36) Schmid, V. H. R.; Thome, P.; Rühle, W.; Paulsen, H.; Kühlbrandt, W.; Rogl, H. *FEBS Lett.* **2001**, *499*, 27−31.

(37) Hayes, J. M.; Matsuzaki, S.; Rätsep, M.; Small, G. J. *J. Phys. Chem. B* **2000**, *104*, 5625−5633.